Dryland avulsion sequences

Insights from data-model comparison of a terminal dryland river system

Karamitopoulos, P.; Donselaar, M. E.; Weltje, G. J.; van Toorenenburg, K. A.

DOI
10.1016/j.sedgeo.2022.106169

Publication date
2022

Document Version
Final published version

Published in
Sedimentary Geology

Sedimentary Geology 436 (2022) 106169

Contents lists available at ScienceDirect

Sedimentary Geology

journal homepage: www.elsevier.com/locate/sedgeo

Dryland avulsion sequences: Insights from data-model comparison of a terminal dryland river system

P. Karamitopoulos [a,b,*], M.E. Donselaar [b,c], G.J. Weltje [c], K.A. van Toorenenburg [b,1]

[a] Delft University of Technology, Department of Hydraulic Engineering, Stevinweg 1, NL-2628CN Delft, Netherlands
[b] Delft University of Technology, Department of Geoscience and Engineering, Stevinweg 1, NL-2628CN Delft, Netherlands
[c] KU Leuven, Department of Earth and Environmental Sciences, Division of Geology, Celestijnenlaan 200E, B-3001 Leuven, Belgium

ARTICLE INFO

Article history:
Received 25 February 2022
Received in revised form 4 May 2022
Accepted 10 May 2022
Available online 13 May 2022

Editor: Dr. Brian Jones

Keywords:
Compensational stacking
Dryland river system
Fluvial geomorphology
Inter-avulsion period
Numerical simulation
River avulsion

ABSTRACT

An advection–diffusion model of fluvial processes was used to analyze the stratigraphic expression of avulsions in terminal river systems and understand their control on basin-fill architecture. The initial and boundary conditions of the model runs (i.e., catchment area, smoothed initial topographic surface, grain-size distribution and sediment supply rates) were extracted from the modern Rio Colorado dryland terminal river system in the Altiplano Basin (Bolivia). Water-discharge and sediment-load values were derived from global regression curves and the *BQART* equation, respectively. To evaluate the robustness of the simulations, the model was tested under increasing sediment-load scenarios ranging from 0.003 m^3/s to 0.095 m^3/s. Data-model comparison provided insights into the role of avulsions in the geomorphological evolution of terminal river systems. The observed stacking of sediments, as captured by geospatial and geochronological data from the Rio Colorado, is consistent with the high sediment-load scenarios, which start with a single-thread fluvial channel that in time radially expands over the floodplain by successive river avulsions on account of alluvial-ridge aggradation and channel-floor elevation above the surrounding floodplain. The model output shows a laterally extensive, convex-upwards lobate topography which is in agreement with the lateral and longitudinal geomorphology in the upper and lower coastal plain of the Rio Colorado. The simulated inter-avulsion period, which is the time period between two successive full (or stabilized) avulsions in the model, varies from 0.18 to 1.2 kyr and is consistent with the OSL-age determination in the Rio Colorado with inter-avulsion periods up to 1.28 ± 0.34 kyr.

1. Introduction

1.1. Introduction

Channel-network evolution in dryland river systems is largely regulated by avulsion dynamics (Kelly and Olsen, 1993; Nichols and Fisher, 2007; Donselaar et al., 2013). Avulsion is a multiscale threshold process that may divert river flow outside the main (or parent) channel toward adjacent low-lying floodplain topography, and thus alter the downstream distribution of fluvial sediments (Leeder, 1978; Bridge and Leeder, 1979; Mackey and Bridge, 1995; Heller and Paola, 1996; Jones and Schumm, 1999; Mohrig et al., 2000; Slingerland and Smith, 2004; Hajek and Edmonds, 2014). Thus, studies of modern and ancient dryland sediments deposited between the gravel–sand transition in the vicinity of orogenic belts and the terminal part of the sediment dispersal system rely heavily on quantitative analysis of the mechanisms and frequency of avulsions (Bryant et al., 1995; Jerolmack and Mohrig, 2007; Donselaar et al., 2022).

Field studies of modern and ancient fluvial systems provide a valuable, yet fragmented record of avulsion recurrences spanning a wide range of spatial and temporal scales (Makaske et al., 2002; Slingerland and Smith, 2004; Aslan et al., 2005; Jones and Hajek, 2007; Stouthamer et al., 2011; Hajek and Wolinsky, 2012; Edmonds et al., 2016). The length of inter-avulsion periods documented in the literature spans up to seven orders of magnitude (10^{-1} to 10^6 yr). Edmonds et al. (2016) suggested that around 60% of recent avulsion events in Andean and Himalayan basins were partial, and that successful (or stabilized) local avulsions take around 11 yrs from initiation to completion. Experimental and field evidence demonstrates that avulsion frequency correlates positively with aggradation rate. The normalized super-elevation (defined as the ratio of alluvial ridge height to channel depth) is a dimensionless measure of a fluvial system's susceptibility to avulsion. The time interval needed to

* Corresponding author at: Delft University of Technology, Department of Hydraulic Engineering, Stevinweg 1, NL-2628CN Delft, Netherlands.
E-mail addresses: P.Karamitopoulos@tudelft.nl (P. Karamitopoulos), m.e.donselaar@tudelft.nl, marinuseric.donselaar@kuleuven.be (M.E. Donselaar), gertjan.weltje@kuleuven.be (G.J. Weltje), Koen.vanToorenenburg@shell.com (K.A. van Toorenenburg).
[1] Present address: Shell International Exploration and Production B.V., P.O. Box 162, 2501AN The Hague, Netherlands.

https://doi.org/10.1016/j.sedgeo.2022.106169

form a deposit of unit thickness, i.e., equal to channel depth, may thus be regarded as a fundamental control on the time evolution of fluvial architecture (Bryant et al., 1995; Heller and Paola, 1996; Jerolmack and Mohrig, 2007). Phillips (2011), Morón et al. (2017), and Nicholas et al. (2018) suggested that the normalized super-elevation at which avulsion is likely to occur decreases in the presence of episodic peak discharges as occurring in dryland fluvial systems.

Dryland fluvial systems are characterized by sparse vegetation, which impacts on the sediment transport process, fluvial morphodynamics and resultant sedimentary architecture (Ielpi and Lapôtre, 2019; Ielpi et al., 2022). The rivers are inactive during prolonged dry periods, which may last from months up to yrs (Garreaud et al., 2003; Li, 2014; Li et al., 2014). Their deposits form during short periods (days) of extremely high precipitation leading to high liquid and solid river discharge. Such peak-discharge events are highly variable in semi-arid regions. In addition, the climate conditions in dryland–river settings imply that the ephemeral channelized flow is subject to transmission losses, owing to large-scale flood-outs out of the channel confinement and onto the floodplain, infiltration and rapid evapotranspiration of excess surface water (Knighton and Nanson, 1994; Lange, 2005; Powell, 2009; Thornes, 2009; Costa et al., 2012; Costa et al., 2013; Donselaar et al., 2013, 2022; Jarihani et al., 2015; Fielding et al., 2018; Henares et al., 2020). Channel-network evolution in dryland river systems is largely regulated by river-avulsion dynamics (Kelly and Olsen, 1993; Nichols and Fisher, 2007; Donselaar et al., 2022). Avulsion diverts river flow from the main (parent) channel toward adjacent sectors of the floodplain, and thus strongly affects the spatial distribution of fluvial sediments deposited downstream of the avulsion point (Leeder, 1978; Bridge and Leeder, 1979; Mackey and Bridge, 1995; Heller and Paola, 1996; Jones and Schumm, 1999; Mohrig et al., 2000; Slingerland and Smith, 2004; Hajek and Edmonds, 2014). In reservoir-geological terms, the thin-bedded fluvial deposits associated with avulsions that are present at the fringes of channel belts and in topographically low sectors of the floodplain are volumetrically important lithofacies units. Their lateral dimensions, internal geometries, and connectivity are poorly resolved by conventional seismic and well-log data, and therefore remain underexplored topics (Nichols and Fisher, 2007; Van Toorenenburg et al., 2016; Colombera et al., 2017; De Jong et al., 2020; Donselaar et al., 2022).

Quantitative analysis of the mechanisms, locations, and frequency of avulsions in dryland–river systems is a prerequisite for capturing the morphodynamic processes and understanding the spatial distribution of channel-belt deposits over time (Bryant et al., 1995; Jerolmack and Mohrig, 2007; Donselaar et al., 2022). Thus, there is a genuine need to investigate the following: (a) the role of river avulsions in geomorphological evolution, (b) the architectural arrangement of channel-belt sediment bodies, and (c) the preservation potential of terminal river systems.

In this study, we present a data-model comparison of the Holocene deposits of the Rio Colorado river system (Altiplano Basin, Bolivia). Satellite imagery, sedimentological and geochronological data were used to set the initial and boundary conditions for a basin-scale advection–diffusion model of fluvial processes (SimClast: Dalman and Weltje, 2008, 2012), and compare its output with the observed deposit geometries. The model was used to simulate the evolution of the medial and distal parts of the dryland fluvial system under different sediment-load scenarios. We used channel-network evolution, fluvial-fan dimensions and estimated inter-avulsion periods as benchmarks for data-model comparison.

1.2. Terminology: avulsion type, style, setup and threshold

In this section we provide a brief history of avulsion-related terminology to clarify the different avulsion terms in this study. Based on numerical experiments with a two-dimensional alluvial stratigraphic model, Leeder (1978) subdivided avulsion behavior (or type) into nodal and random. The former originates from a relatively fixed area on the floodplain, whereas the latter may occur anywhere along the active channel. Heller and Paola (1996) characterized avulsions as local or regional based on the downstream distance over which the newly-formed channel remains outside its former course. Slingerland and Smith (2004) recognized full (also termed successful or stabilized) and partial avulsions based on whether the entire flow, or only a portion of it, is transferred out of the main channel, respectively. They also summarized three avulsion style end-members based on distinct floodplain responses: (1) avulsion by annexation, in which a channel is captured or reoccupied, (2) avulsion by incision, and (3) avulsion by progradation. Hajek and Edmonds (2014) quantified the intermediate states between incisional and progradational avulsion styles while also underscoring the significance of floodplain morphodynamics to condition sedimentation patterns in avulsive systems. Mohrig et al. (2000) summarized avulsion setup in terms of two different measures: (a) levee growth, which increases the ratio of cross-floodplain to along-river gradients, and (b) superelevation, which '*calculates the relief between the water-surface elevation in a channel at bankfull discharge (i.e., levee height) to the minimum elevation of the adjacent flood plain (Heller and Paola, 1996). It is possible that these two measures are correlated if levee slope becomes steeper as the total amount of superelevation increases, such as in the model of Slingerland and Smith (1998)*'. Avulsion thresholds control avulsion initiation and may either refer to short term (annual to decadal) conditions under which a bifurcation or crevasse channel becomes stable or to long-term conditions that cause a full regional avulsion at landscape/architecture scale (Hajek and Wolinsky, 2012). After avulsion initiation, the distributed flow adjacent to the parent channel will seek for gradient advantage on the floodplain (Hoyal and Sheets, 2009; Reitz et al., 2010). Ultimately, the stabilization of a newly-formed crevasse channel is achieved by the appropriate combination of local conditions (i.e. cross-channel flow potential exceeding a certain threshold level, bed geometry at bifurcation sites, factors favoring floodplain incision) and an optimal downstream path at landscape-scale (Slingerland and Smith, 2004; Kleinhans et al., 2013; Hajek and Edmonds, 2014; Edmonds et al., 2016; Nienhuis et al., 2018). Finally, Jones and Schumm (1999) subdivided the conditions necessary for an avulsion into two main groups (or setups): (a) a long-term setup in which the channel gradually increases its susceptibility to avulsion and (b) a short-term trigger that initiates the avulsion (i.e. episodic peak discharges).

2. Data and methods

2.1. Field area and avulsion history

The Altiplano Basin is a high-altitude (3650–4200 m), internally drained (endorheic) semi-arid basin, filled by Cretaceous to Holocene fluvio-lacustrine and eolian sediments (Donselaar et al., 2013; Li et al., 2014). The basin is in a tectonically quiescent phase since the onset of the Holocene, with only minor vertical uplift at a rate of 0.2 to 0.3 mm/yr (Gregory-Wodzicki, 2000). The Holocene history of the modern Rio Colorado dryland river system in the Altiplano Basin (Bolivia) has been reconstructed in detail (Donselaar et al., 2013, 2022; Li, 2014; Li et al., 2015; Van Toorenenburg, 2018; Van Toorenenburg et al., 2018). The system provides a suitable analog for our study as it has undergone limited anthropogenic modifications. Analysis of satellite imagery, sedimentology, and geochronology of the Rio Colorado enabled the sequential reconstruction of the sediment routing system between the west flank of the Andean Cordillera Oriental and the terminal part of the sediment dispersal system, where the river ends on the salt flat bordering the Salar de Uyuni salt lake (Fig. 1).

The total drainage area of the Rio Colorado is ca. 15,000 km^2 (Donselaar et al., 2013), and the river is subdivided into five sections from source to sink: (1) upstream section with small tributary channels, (2) confined river in a narrow gorge, (3) steeply-dipping alluvial-fan

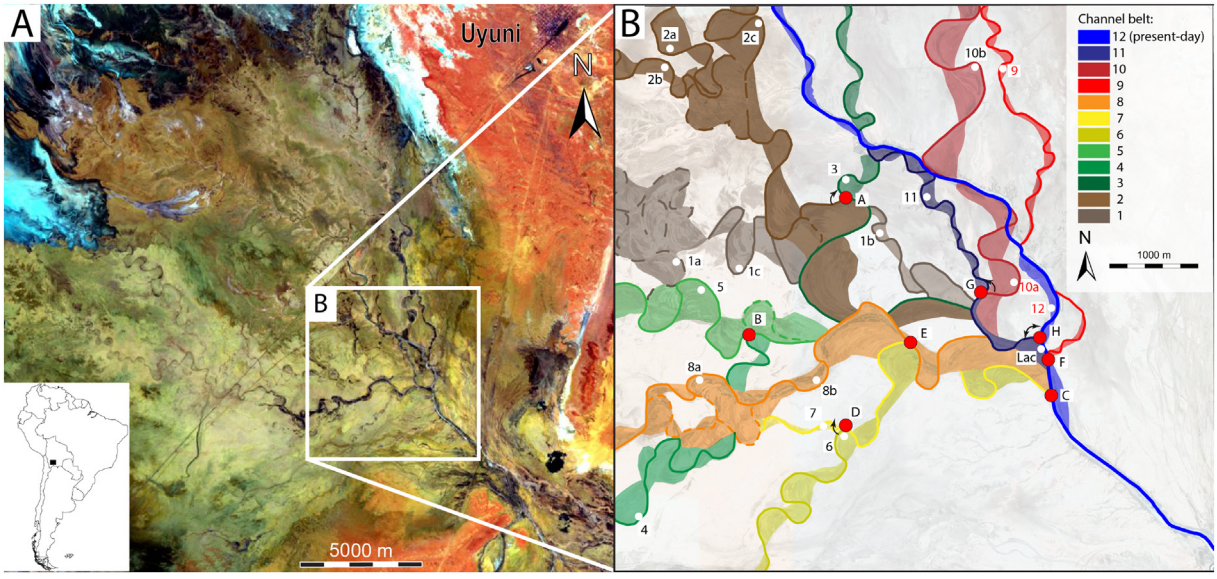

Fig. 1. (A) Landsat-7 ETM+ image (band combination 5, 3, 1) of the divergent terminal part of the Río Colorado river system; image date is 16 Nov. 2002. Flow is toward the NW. White–blue-brownish colors: edge of the Salar de Uyuni (modified after Donselaar et al., 2013 and Donselaar et al., 2022). (B) Reconstruction of channel-belt evolution in space and time, based on satellite imagery analysis and OSL dating of sediment samples (labeled white dots 1 to 12, Lac) in the different channel-belt deposits. Relative geochronological order indicated by different colors. Labeled red dots: avulsion points A to H. From: Donselaar et al. (2022).

(bajada), (4) upper coastal plain with straight midstream river section, and (5) meandering-river section in the lower coastal plain (Fig. 2A).

Discharge events in the study area typically last 24–48 h, with peak discharges exceeding 100 m^3/s (Donselaar et al., 2013; Li, 2014). The volume of floodwater in periods of peak discharge by far exceeds the capacity of the river to maintain the flow within its channel banks. Hence, large-scale flood-outs occur, with formation of levees, crevasse-channel, crevasse-splay and terminal-splay deposits along the trunk river. Aggradation of these deposits to an alluvial ridge leads to the decrease of the along-river gradient and simultaneous increase of the cross-floodplain gradient, which favors the initiation and stabilization of river avulsions (Mohrig et al., 2000; Donselaar et al., 2013, 2022; Li, 2014; Van Toorenenburg et al., 2018). The in-channel gradient of the lower lacustrine coastal plain is extremely low (1:12,000), fluvial incision is minimal to absent, and channel width and depth decrease downstream (Donselaar et al., 2013).

Successive Rio Colorado river paths all started with a low to moderately sinuous (SI 1.25 to 1.58) trajectory bordered by small lateral bars,

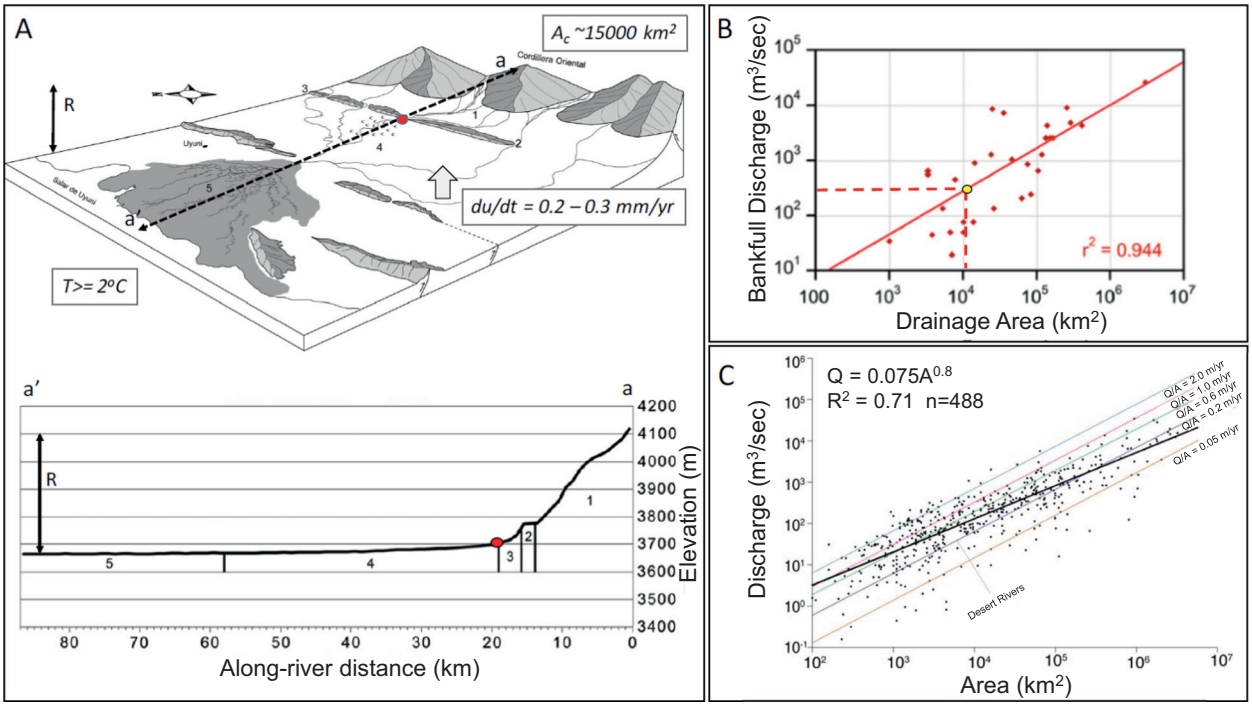

Fig. 2. (A) Block diagram of the Rio Colorado river system (top) and along-river profile with five river path segments (bottom) (modified after Donselaar et al., 2013). (B) Global regression curve of estimated water discharge as a function of drainage area (modified after Blum et al., 2013). Yellow point indicates environmental parameters for Altiplano Basin. (C) Basin-averaged discharge and its power-law relationship with drainage area (after Syvitski and Milliman, 2007).

and gradually evolved into highly sinuous (SI 1.70 to 2.56) streams by point-bar lateral accretion (Donselaar et al., 2022). The geochronology of the river avulsions, and the mean inter-avulsion period were established with optically stimulated luminescence (OSL) dating of 18 sediment samples, collected in shallow pits at the interface of the last point-bar lateral-accretion deposits with the abandoned-channel fill, thus capturing the time of abandonment of the river path. Intra-avulsion periods are up to 1.28 ± 0.34 kyr. The present-day path of the Rio Colorado river system initiated by avulsion at 0.62 ± 0.13 kyr BP (Donselaar et al., 2022). The resultant landform of the lower coastal plain has a convex-upward lobate shape, formed by a network of compensationally-stacked alluvial ridges (Friend et al., 1979; North and Warwick, 2007; Li et al., 2015; Van Toorenenburg, 2018; Donselaar et al., 2022). The fluvial deposits in the lower coastal plain attain a maximum thickness of 3 m and an areal extent of ca. 500 km^2 (Fig. 1A). They overlay diatom-rich lacustrine clays that formed during the last lake-level highstand, which ended 11.5 kyr BP (Baker et al., 2001; Blard et al., 2011).

2.2. Model description

The synthetic stratigraphy in this study was acquired using SimClast, a model developed by Dalman and Weltje (2008). The model is capable of simulating channel network dynamics, floodplain interactions and coastal processes. The fluvial module of SimClast simulates channel-network development through the routing of dispersive flow on the floodplain (Freeman, 1991; Meijer, 2002), and advective transport in channels. River avulsions are simulated by using a simplified bifurcation-stability routine (Slingerland and Smith, 1998). A central assumption in the model is that channel-belt aggradation locally increases the ratio of cross-floodplain to in-channel gradients and thus creates favorable conditions for avulsions to occur (Slingerland and Smith, 1998; Jones and Schumm, 1999; Mohrig et al., 2000; Aslan et al., 2005; Hajek and Wolinsky, 2012; Hajek and Edmonds, 2014; Edmonds et al., 2016; Ganti et al., 2016; Nicholas et al., 2018; van Toorenenburg et al., 2018). Crevassing (or levee breaching) is regarded as a spatially random triggering mechanism conditioned by local topography that initiates channelized flow outside the parent channel. The stability of a newly-formed channel is determined by estimating the equilibrium water discharge (which is redistributed over the old channel and the crevasse channel) and corresponding sediment transport capacity of the crevasse channel, based on the vertical sediment concentration gradient in the parent channel. If sediment load exceeds transport capacity, the river bank of the parent channel will heal. Conversely, the crevasse channel will evolve by incision until its transport capacity balances the sediment load (Fig. 3). This approach permits simulation of a variety of phenomena characteristic of drainage network evolution: failed avulsions, stable bifurcations, full avulsions, and channel-belt re-occupation (Dalman and Weltje, 2008; Karamitopoulos et al., 2014).

2.3. Model boundary conditions for numerical simulation

Mass balance and scale analysis enabled the approximation of the boundary conditions for the simulations, which comprise base (lake) level and rate of sediment supply. The water-discharge (Q_w) and sediment-load (Q_s) values were derived from global regression curves (Blum et al., 2013) and the *BQART* equations (Syvitski and Milliman, 2007), respectively (Fig. 3). Based on the regression of Q_w on catchment area (A_c), a water discharge of 500 m^3/s was derived. This estimate lies in the same order of magnitude with the peak discharge obtained by model-based ratings (https://floodobservatory.colorado.edu/) and the input water discharges used in a previous modeling study of an analogous river system in Lake Eyre Basin, Australia (Morón and Amos, 2018).

Sediment load (or yield) was estimated using a variation of the *BQART* model (Syvitski et al., 2003; Syvitski and Milliman, 2007; Kettner et al., 2010; Cohen et al., 2013; Weight et al., 2011; Allen et al., 2013; Sømme et al., 2013; Zhang et al., 2018; Brewer et al., 2020):

$$Q_s = \omega B Q_w^{0.31} A^{0.5} RT \quad (1)$$

where Q_S is sediment load, ω is equal to 0.0006, Q_W is the estimated water discharge, B is the anthropogenic-geological influence factor (set equal to 1 since human influence, glacial influence and water trapping are negligible), R is the catchment maximum relief (ca. 0.45 km) and T is basin-averaged temperature (≥2 ° C). By using these values, Q_S was found equal to 0.23 km^3/yr (7.29 m^3/s). We assumed that only a small fraction of the estimated sediment load (≤1%) reaches the upstream apex of the system owing to high rates of water loss and great variability in water discharge from the drainage basin to the sediment entry point of the system. This assumption is consistent with a rudimentary volumetric approximation using a fan area of ~500 km^2 and an average thickness (~1 m). The product of area and thickness is equal to 0.5 km^3. Assuming that the Rio Colorado river system has been active for at least 3.69 ± 0.34 kyr (age of oldest abandonment), the ratio of volume over this minimum age yields an averaged Q_S on the order of 10^5 m^3/yr (or 10^{-4} km^3/yr).

Fluvial system evolution was simulated under time-invariant external forcing for a period of 4000 yr, which approximates the age of the oldest abandoned river path (Channel belt 1) in the study area (Donselaar et al., 2022). The grid cell size was set equal to 1 × 1 km and the time step to one yr, which represents the finest spatio-temporal resolution at which the model can operate (Dalman and Weltje, 2008). For all experiments, we assumed that Q_w and Q_s are averaged over the course of each time step. Bifurcation and avulsion dynamics were tested under a wide range of sediment load scenarios (0.003 to 0.095 m^3/s) in order to evaluate the robustness of the model results and fine-tune the model input.

The different scenarios were named in terms of increasing sediment load (SL): SL1, SL2, SL3, SL4 and SL5 correspond to solid river discharge of 0.003, 0.015, 0.03, 0.06 and 0.095 m^3/s respectively. In each SL scenario, water and sediment were supplied at a constant rate to the upper coastal plain of the basin through a single entry point representing the boundary between the steeply-dipping alluvial fan segment and the upper coastal plain. The initial topographic surface of model was set equal to 0.0015 in order to account for the higher gradient of the upper coastal plain of the Rio Colorado river system. Sandy and muddy sediments (with a fixed grain-size distribution of 20% and 80% of each by volume) were represented by two grain-size end-members (0.5 mm and 0.0001 mm, respectively) in accordance with grain-size distributions of samples in the study area (Li et al., 2015). The grain-size distribution of the subsurface was set to be identical to the sediment feed.

2.4. Quantification of system response

Bifurcation events and avulsion occurrences were extracted from the model output. For every time step, dynamic parameters representative of water flow and sediment transport were estimated. One of the parameters is the cross-sectional area a, which is the wet area of channel cross section at mean volumetric flow rate (Q), derived from an expression of the mass (and volume) conservation equation:

$$Q = u_1 a_1 = u_2 a_2, \quad (2)$$

where u is decomposed, and represented by mean flow velocity. This is an empirical equation (also known as Darcy–Weisbach equation) which relates pressure loss due to friction along a given length of a pipe to the average velocity of the fluid flow for an incompressible fluid. The equation is useful in the transition region between laminar flow and fully-developed turbulent flow. It contains a dimensionless friction factor (f_D) which was assumed to be equal to 0.05, representative of sand-bed rivers. Another parameter which was estimated during the model runs is the aggradation to progradation (A/P) ratio which is

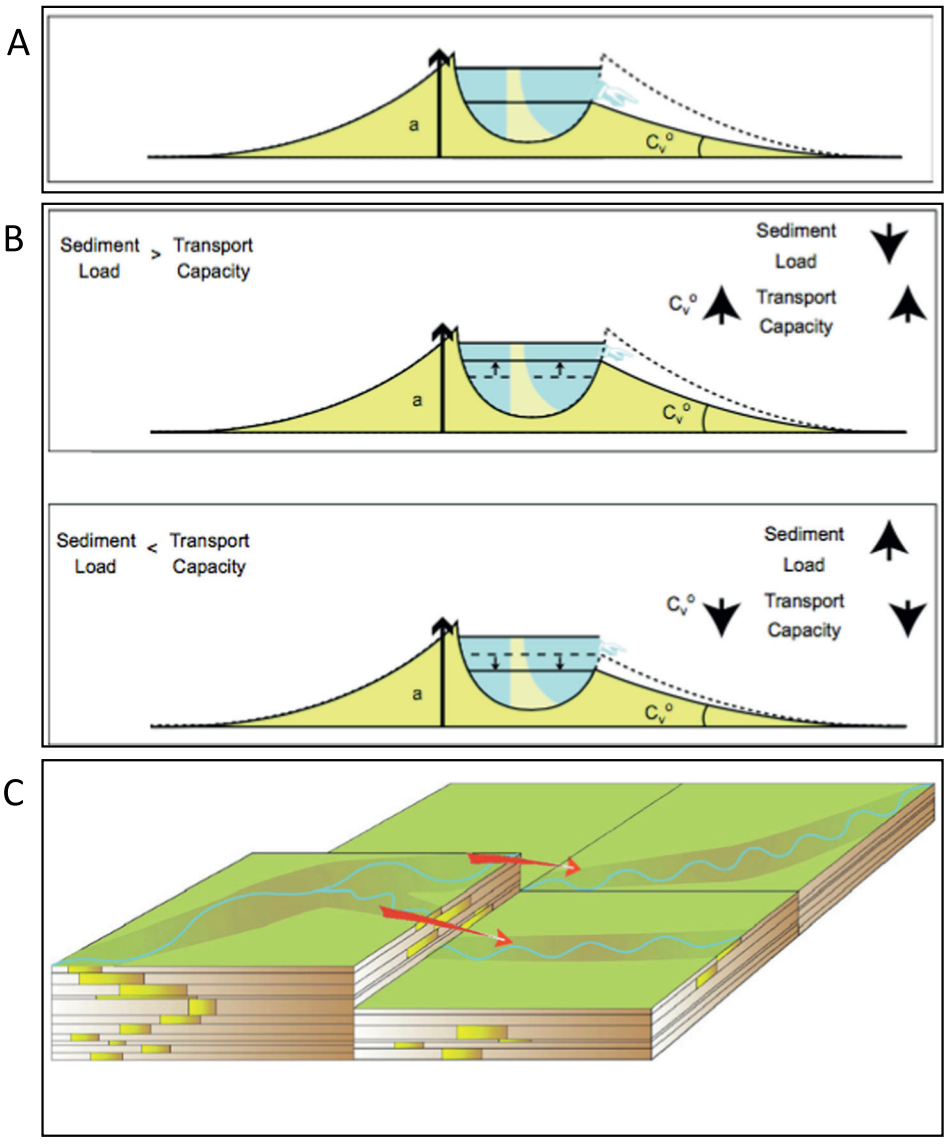

Fig. 3. SimClast avulsion rules: (A) initiation by crevasse triggering, (B) conditions for crevasse termination (sediment load exceeds transport capacity) or stabilization (transport capacity exceeds sediment load). (C) Oblique view of stabilized channel network after successful crevassing.
(Modified after Dalman and Weltje (2008).)

indicative of alluvial aggradation and equals the thickness ratio of net sediment deposited above base level to net sediment deposited below base level across the entire grid (Fig. 4).

The geomorphic end-products of the numerical experiments consist of multiple topographic maps and visualizations of sedimentation pattern and water discharge. Post-processing of the stratigraphic and water discharge output of the model enabled: (1) the clustering of channel deposits into avulsion-based river pathways (or tracts), (2) the quantification of flow occupancy defined by the percentage of simulation time a grid cell was occupied by an active channel (Ashworth et al., 2007; Van Dijk et al., 2009), and (3) calculation of the cumulative volume of total aggradation. Finally, the normalized inter-avulsion period was defined as the inter-avulsion period divided by the total period of the record (Mackey and Bridge, 1995).

3. Results and discussion

The low sediment load scenarios ($Qs \leq 0.03$ m^3/s) are characterized by straight channels and fixed drainage to the terminal part of the sediment dispersal system where symmetrical lacustrine deltas grow by means of mouth bar-induced bifurcation events at the terminus (Fig. 5A). The geomorphic pattern changes over time in the high sediment load scenarios ($Qs > 0.03$ m^3/s) as a consequence of higher rates of alluvial-ridge aggradation, deposition of higher-sinuosity channel-belt sediments and increase of cross-floodplain gradients. Such conditions favor the initiation and stabilization of avulsions (Fig. 5B).

In the early stage of the high-load scenario (SL5), channels remained in place for long periods of time acting mostly as conduits for sediments to reach the coastline (Fig. 6A). The emergent avulsive behavior during later stages led to dispersion and offset stacking of sediments across the floodplain forming a laterally extensive convex-upwards lobate topography with abandoned channel deposits arranged on either side of the main paleoflow axis (Fig. 6B).

The second part of the work focused on the comparative analysis of the modeled and observed avulsion behaviors. Avulsions extracted from SL5 are organized in three sequences (Fig. 7). Each sequence groups a series of avulsion sites that shift progressively upstream with a concomitant decrease in avulsion periodicity (Mackey and Bridge,

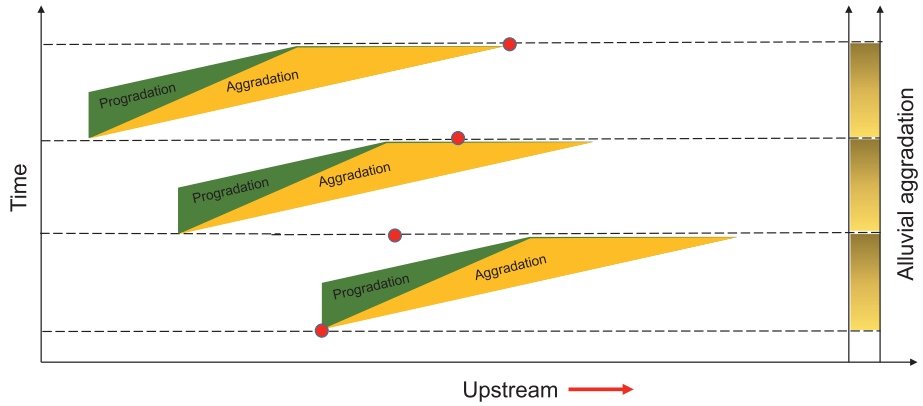

Fig. 4. Definition diagram of A/P ratio. Each depositional episode starts with progradation of lower coastal-plain facies and/or delta lobes and concomitant aggradation of upper coastal-plain and fluvial facies. Note upstream migration of avulsion sites (red dots) forming the apex of the delta.

1995; Stouthamer et al., 2011). The avulsions extracted during SL5 allowed the subdivision of the simulated stratigraphy into 22 river tracts (or flow paths) and their associated deposits (Fig. 8A). Avulsions that fell below the temporal resolution limit of the morphodynamic output (40 yr) were grouped in the same cluster. Avulsions included full (or stabilized), partial and failed avulsions. Post-processing of the channelized drainage evolution permitted the estimation of flow occupancy (Fig. 8B, C). The normalized avulsion periods are based on a normal kernel function evaluated at equally-spaced points covering the entire range of observed and modeled data (Fig. 9). The last three parts of the section focused on the architectural arrangement of a dryland fluvial succession and the preservation potential of the associated deposits.

3.1. Morphodynamic evolution

For all experiments, we took a regionalized approach by assuming that Q_w and Q_s are averaged over the course of each time step. In reality, more than 95% of the annual discharge arrives within a few days in short, high-magnitude peak-discharge events (Garreaud et al., 2003; Li, 2014). The greatest limitation of this approach is the uncertainty related to the magnitude and spatial distribution of rainfall

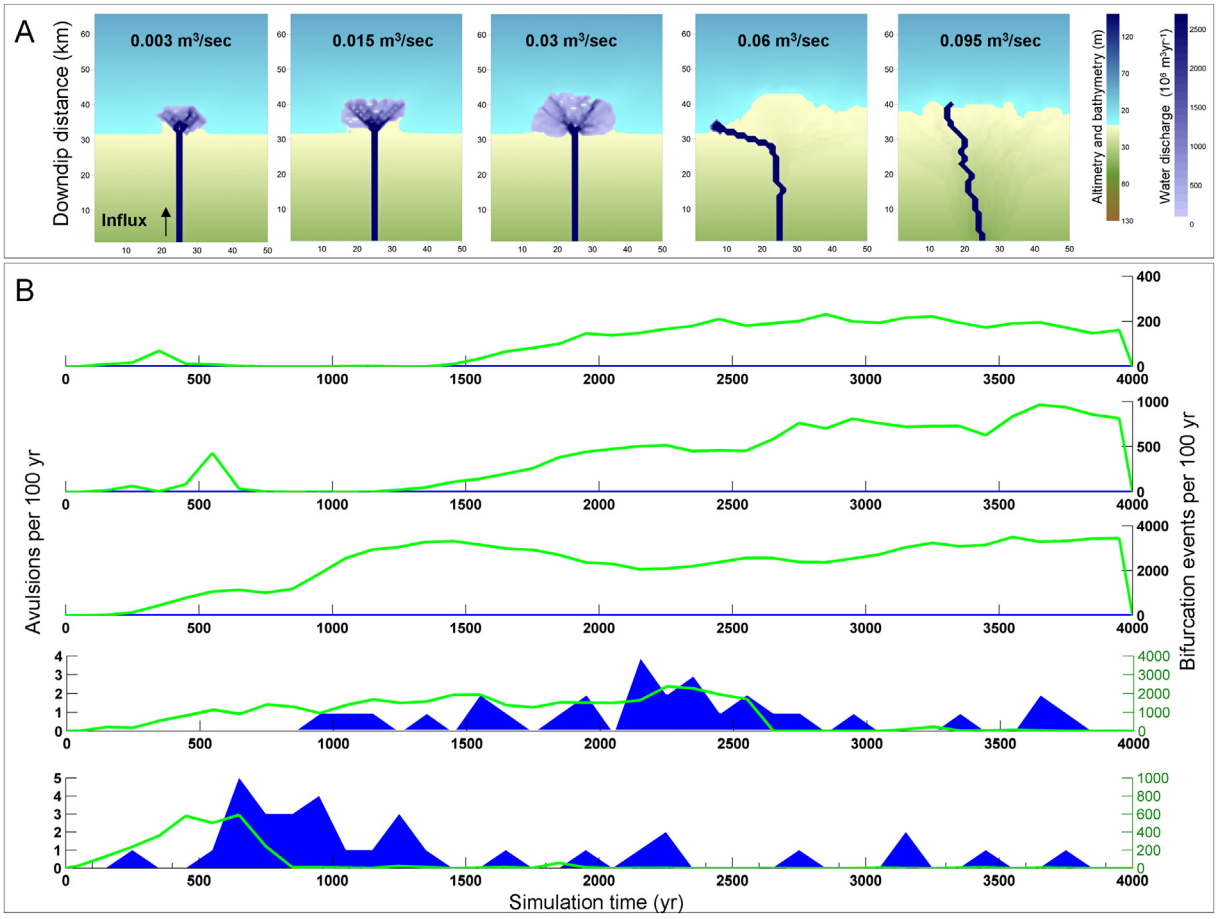

Fig. 5. (A) Plan-view morphology snapshots of all numerical experiments (scenarios SL1 to SL5 from left to right). (B) Total avulsion occurrences (blue area) including full, partial and failed ones and bifurcation events (green line) per 100 yr.

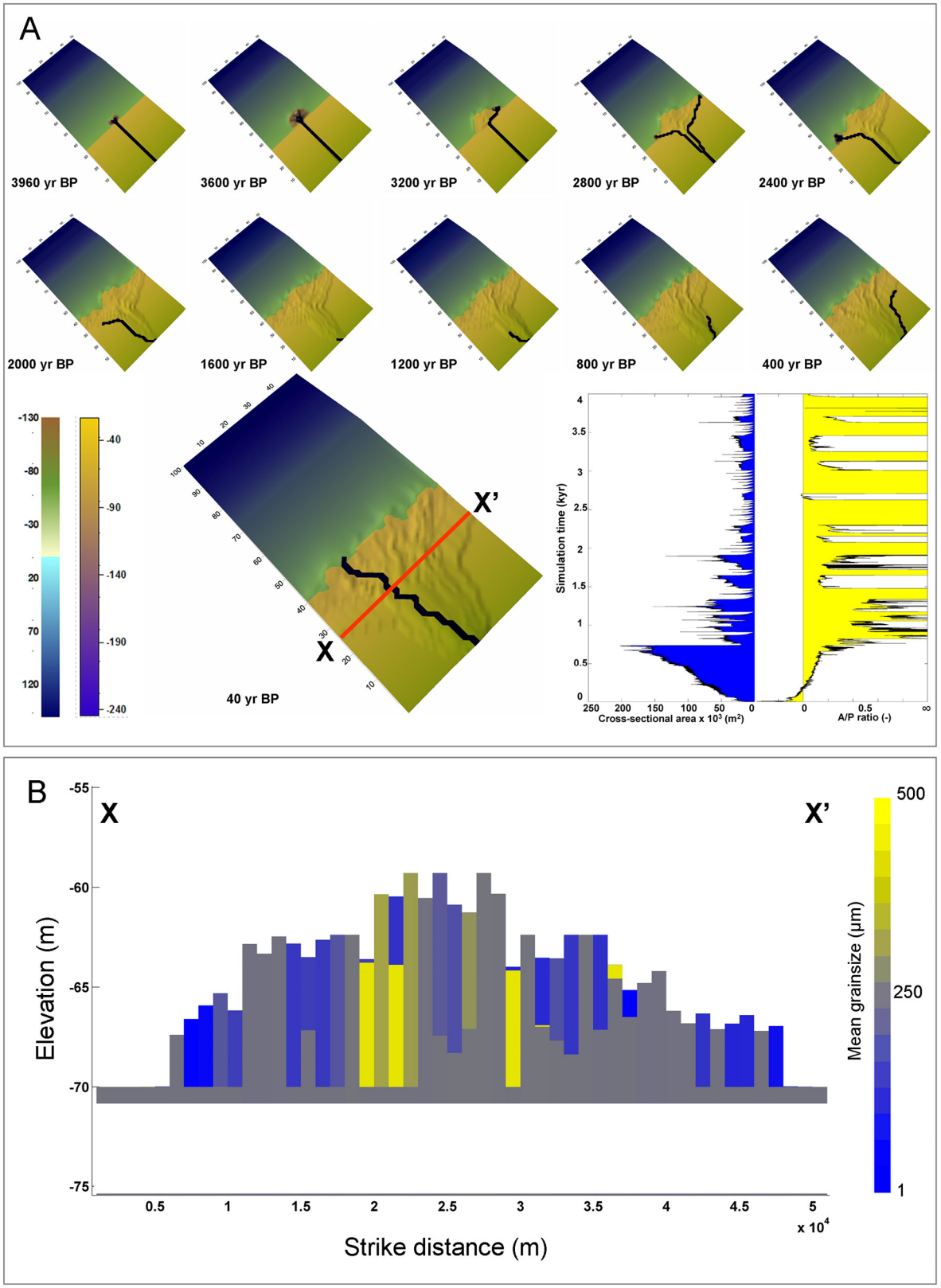

Fig. 6. (A) Snapshots of simulated morphodynamic evolution of the high load scenario SL5 (altimetry and bathymetry scales are superimposed for topographic relief intonation), inset: cross-sectional area and aggradation/progradation (A/P) ratio curves (see text for more details). (B) Strike section of synthetic stratigraphy (~25 km downdip) represented by median grain sizes.

which is a common problem when interpolating hydrological information to ungauged catchments (He et al., 2011). Water loss by flood-outs, infiltration and evapotranspiration impose additional uncertainties. Our simplified approach to regionalize streamflow properties directly avoids these issues (de Lavenne et al., 2016) because examination of causal rainfall–runoff relations is not within the remit of this study.

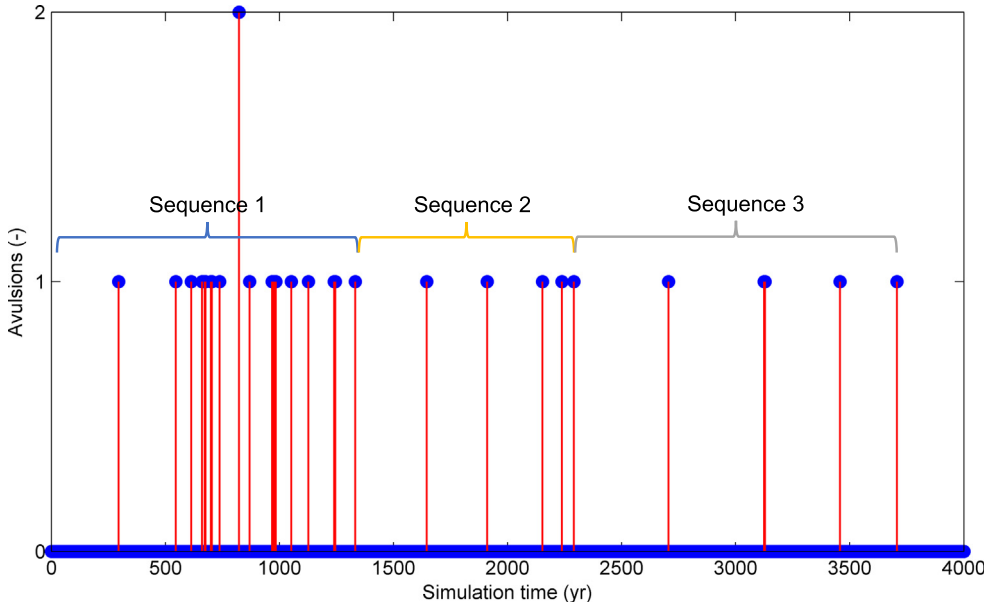

Fig. 7. Extracted avulsion events (including full, partial and failed avulsions) and interpreted avulsion sequences. Time period between two successive occurrences marks the total inter-avulsion time that is available for alluvial-ridge aggradation.

The model output illustrates the relationship between morphodynamic evolution and the dominant spatio-temporal patterns of sedimentation (Fig. 6A). During the first stage of the simulation (4000–3200 yr BP), deposition is strongly progradational and marked by a rapid increase of the cross-sectional channel area (Fig. 6A, inset). Under constant discharge rate, sediments reach the distal part of the lower coastal plain forming a symmetrical lacustrine delta. At ca. 3200 yr BP, the system is punctuated by a significant decrease in the cross-sectional channel area. The longitudinal outbuilding of the system lengthens its fluvial profile, reduces equilibrium gradient and induces upstream aggradation (Dalman et al., 2015). This in turn increases the cross-floodplain gradient relative to the slope downstream and prepares the ground for an avulsion which can be initiated by a flooding (or crevassing) event (van Toorenenburg et al., 2018; Donselaar et al., 2022). In case of a full avulsion, the newly-formed channel incises into the surrounding floodplain area while a juvenile lobate unit is deposited on a topographically lower-lying area downstream. The channels are backfilled with sediments and set up the system anew to an avulsion prone state.

3.2. Data-model comparison and avulsion thresholds

The data-model comparison, which was conducted on the basis of channel-belt network evolution, the fluvial-fan geometry and probability density estimates of normalized avulsion periods, showed that the observations in the Altiplano Basin are in accordance with the high sediment-load scenarios (Figs. 1, 2, 5A, 6A, B, 8). The successive Rio Colorado river paths all started with a moderately-sinuous (SI 1.25 to 1.58) trajectory bordered by small point bars, and gradually evolved into highly-sinuous (SI 1.70 to 2.56) streams with wide point bars with a large surface area (Donselaar et al., 2022). This is consistent with the modeled channelized flow (scenarios SL4 and SL5), which started with a straight single-thread channel and over time switched radially on account of continuous growth of alluvial ridges, deposition of higher-sinuosity channel-belt sediments, and the gradual increase of the ratio of cross-floodplain to along-river gradients. Compensational offset stacking of sediments formed a convex-upwards lobate topography which extends ca. 10 km in the proximal part, ca. 50 km in the distal part and is a few meters thick (2–5 m and 2–12 m for scenarios SL4 and SL5, respectively). Higher slopes occur in the vicinity of the main paleoflow axis with a gradual decrease toward down-valley direction. These dimensions are comparable to the lateral and longitudinal extent of the fluvial forms in the upper and lower coastal plain of the Rio Colorado river system.

The normalized avulsion periods are based on a normal kernel function evaluated at equally-spaced points covering the full range of observed and modeled data (Fig. 9). For the simulated scenarios, the avulsion threshold between the failed/partial avulsions and the full ones was defined by the intercept of the first two peaks of the probability distributions (~0.045, which equals an avulsion period of 180 yr). The simulated avulsion periods in scenario SL4 range from 180 to 1200 yr (corresponding to 0.045 and 0.3 normalized avulsion periods, respectively), whereas the estimated inter-avulsion periods in the study area range from 400 to 1300 yr. The model results include a large number of failed/partial avulsions, which is likely not the case for the observed data, as these reflect full avulsions only. Evidence of failed/partial avulsions in the outcrop analog study tends to be obscured by the subsequent evolution of the system which includes expansion of the alluvial ridges and partial erosion of previous river paths. Comparative analysis between scenarios SL4 and SL5 shows that a potential increase in sediment load (i.e. scenario SL5) shifts avulsion recurrences to a higher-frequency domain.

3.3. Avulsion sequences

Avulsions in the high sediment-load scenarios are organized in three sequences (Fig. 7). Each sequence groups a series of avulsion sites that shift progressively upstream with a concomitant decrease in avulsion periodicity. In the first stage, deposition is strongly progradational with predominantly bifurcation events occurring at the lacustrine delta edge and a few nodal and local avulsions. The gradual lengthening of the fluvial profile reduces equilibrium gradient and induces upstream aggradation which marks the initiation of a new avulsion sequence which drives depocenter shifts to adjacent regions partially onlapping onto older existing fluvial fans or toward a completely new course driven by regional avulsions. During the last stage, sediment is fed from random avulsions into the surrounding topographic lows while avoiding the previously formed alluvial ridges. Episodic peak discharge periods generate the sediment fluxes necessary to trigger the last stage

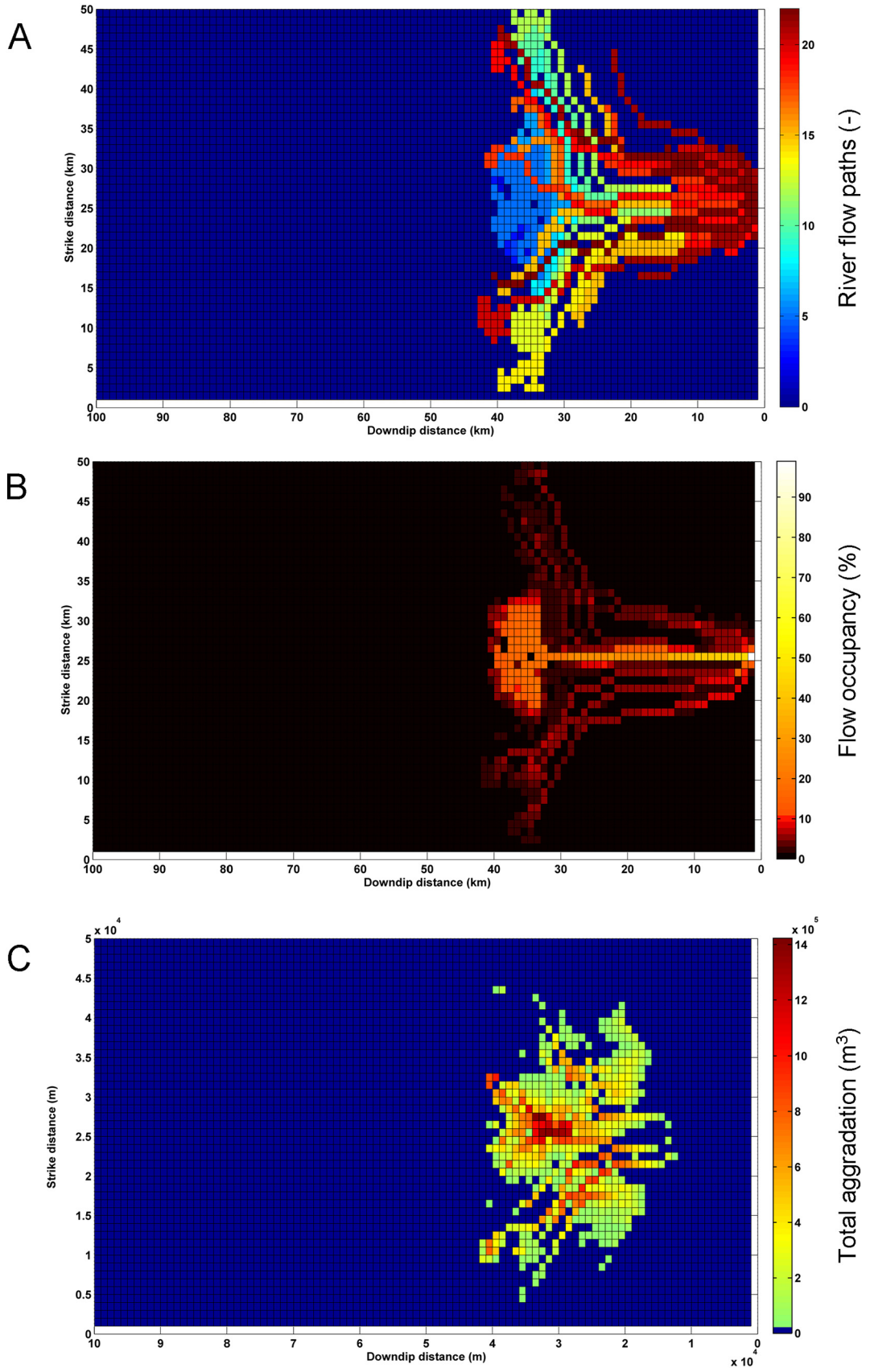

Fig. 8. (A) Successive river flow paths. (B) Estimated flow occupancy. (C) Total aggradation.

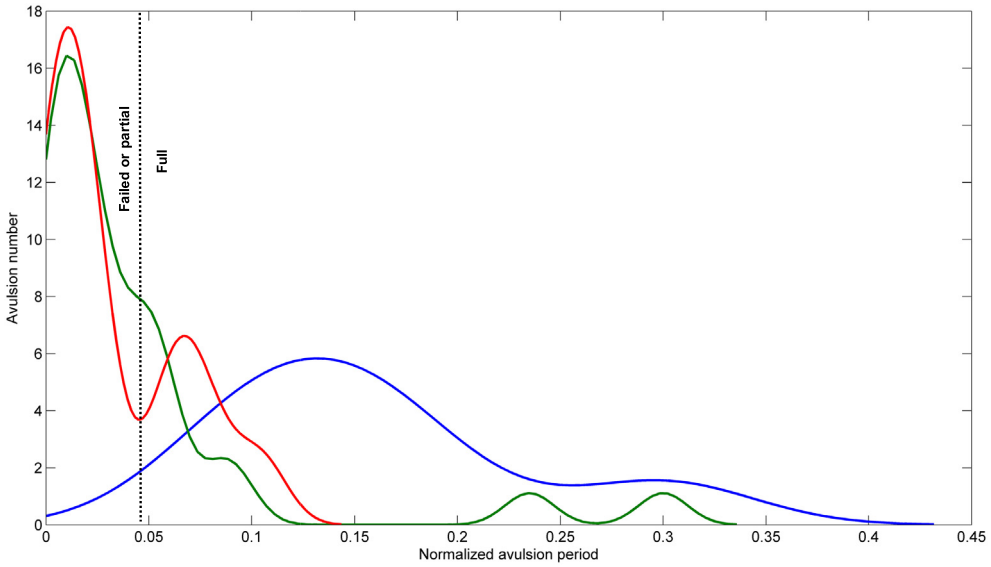

Fig. 9. Probability density estimates of normalized avulsion periods for the observed (blue) and modeled periods. Green and red lines correspond to scenarios SL4 and SL5 respectively. Black dotted line indicates boundary between partial or failed avulsions and the full (stabilized) ones. (For interpretation of the references to color in this figure legend, the reader is referred to the web version of this article.)

as described above owing to excessive amounts of rainfall in the drainage area forcing rapid flooding events. This is supported by the analysis of remote sensing imagery over the period of 30 yr which suggested that morphological changes at the terminus of the Altiplano system occur after peak discharge events (Li et al., 2018).

3.4. Architecture of dryland fluvial successions

Various hypotheses, supported by morphodynamic modeling and field studies, gave new insights about the formation and architectural arrangement of channel-belt sediment bodies (Leeder, 1978; Bridge and Leeder, 1979; Mackey and Bridge, 1995; Kraus and Aslan, 1999; Mohrig et al., 2000; Gouw, 2007; Hajek et al., 2010; Wang and Plink-Björklund, 2019). In this study, the spatial organization of the abandoned channel belts reflects the adjustment of active river tracts to the inherited (local) base level by compensational stacking (Sheets et al., 2002; Straub et al., 2009; Wang et al., 2011; Hajek and Wolinsky, 2012; Edmonds et al., 2016). Over time, the initial single-thread channel gradually expands radially into multiple channels on account of continuous growth of alluvial ridges and avulsion-induced compensational stacking. The channel belts diverge over the unconfined floodplain area where reworking is less likely to occur. The resulting depositional architecture is a laterally extensive sheet with a fan-shaped top view and a convex-up shape, made up of radially arranged, connected sandy alluvial ridges (Fig. 10). Recent field research focusing on crevasse-splay architectural elements in the same area concluded that avulsion initiation is favored locally by alluvial-ridge development associated with compensational stacking of crevasse-splay deposits and channel-floor elevation above the floodplain (Van Toorenenburg et al., 2018; Donselaar et al., 2022).

3.5. Preservation of a terminal fluvial system

Over the short term, the spatial variation in flow occupancy plays a key role in the sedimentation and preservation of the fluvial-fan channel deposits (Fig. 8). Long flow-occupancy periods in the proximal area correspond to low total aggradation because the conveyor belt constantly reworks and distributes sediment downstream (Fig. 8C). By contrast, higher abundance of channel-belt volumes is found across the medial to distal areas. This is consistent with previous experimental observations of channelized flows that occupy a particular route in the basin without filling it (Sheets et al., 2002; Ashworth et al., 2007; Van Dijk et al., 2009). Short-term sequestration and preservation run against common stratigraphic evidence which suggests that high relative volumes of channel deposits typically lie in the proximal sectors of fluvial-fan bodies. Therefore, we distinguish between topographic fluvial fans, which are fans defined by surface topography at some instance in time, and the final preserved fluvial fans in the stratigraphic record. Over the long term, the preservation of sediments of the terminal fluvial system is regulated by the regional subsidence pattern, and therefore periods of base-level rise (Miall, 1996). Under stable base-

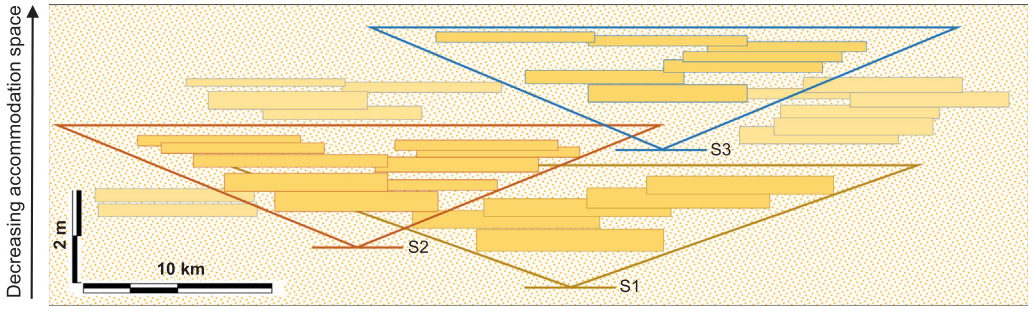

Fig. 10. Conceptual model of alluvial architecture illustrating a medial-to-distal cross-section. S1, S2 and S3 represent clusters of channel-belt sediment bodies (yellow) corresponding to the three successive stages of dryland avulsion sequences. Background represents fine-grained deposits.

level conditions, the progradation of the terminal fluvial system may be translated into a fixed rise of base level across the entire coastal plain which induces aggradation upstream (Dalman et al., 2015). Additional accommodation may be provided by the higher compaction rates of floodplain fines relative to the coarser grain-size fraction. By contrast, intense floods may abruptly destroy accommodation and generate recognizable sedimentary signals in sink areas (i.e., storm intensity correlatable to mean grain size signature; Romans et al., 2016). Finally, in the case of a high-magnitude base level rise, low-stand fluvial fan deposits simply drown owing to enclosed basin conditions with minimal wave action and along-shore currents and are draped with lacustrine high-stand mud (De Jong et al., 2020).

4. Conclusions

An advection–diffusion model of fluvial processes allowed us to analyze the following: (a) the role of river avulsions in geomorphological evolution, (b) the architectural arrangement of channel-belt sediment bodies, and (c) the preservation potential of terminal river systems. Geospatial and geochronological data from Rio Colorado Data enabled comparisons with the model output. The observed offset stacking of sediments in the river system is consistent with the high sediment-load model scenarios, which started with a single-thread channel, and in time expanded radially into multiple channels on account of progressive growth of alluvial ridges and avulsion-induced compensational stacking. The geomorphic end-product is a convex-upwards lobate topography with a thickness of a few meters, and abandoned channel deposits on either side of the main paleoflow axis that extends over 10 km in the proximal part, and 50 km in the distal part of the terminal river system. The modeled geomorphology shows a good comparison with the geomorphology in the upper and lower coastal plain of the Rio Colorado river system. The simulated avulsion periods of the high sediment-load scenario (180–1200 yr) show a good match with the avulsion periodicity of 1.28 ± 0.34 kyr in the Rio Colorado river system.

The model output yielded three successive stages of river evolution, which determine the resultant landform in this study: (1) rapid river progradation with bifurcation events at the lacustrine delta edge, and a few nodal and local avulsions; (2) gradual lengthening of the fluvial profile, which reduces equilibrium gradient and induces upstream aggradation, and triggers new avulsions that result in depocenter shifts to adjacent low-lying regions; and (3) compensational stacking in topographic lows in between alluvial ridges by random local avulsions. The integrated approach of process-based modeling in combination with geospatial and geochronological data sets provides a large-scale framework for modeling studies of ancient fluvial stratigraphic units in which the radial extent of the fluvial system and the spatial organization of its isolated channel-belt sediment bodies are controlled by avulsion-induced compensational stacking.

Declaration of competing interest

The authors declare that they have no known competing financial interests or personal relationships that could have appeared to influence the work reported in this paper.

Acknowledgements

The authors are grateful for the constructive reviews by Nigel Mountney and Jörg Lang. Rory Dalman and Dario Ventra are gratefully acknowledged for their helpful comments on earlier versions of the manuscript. Brian Jones is thanked for the excellent handling of the manuscript.

References

Allen, P.A., Armitage, J.J., Carter, A., Duller, R.A., Michael, N.A., Sinclair, H.D., Whitchurch, A.L., Whittaker, A.C., 2013. The Qs problem: sediment volumetric balance of proximal foreland basin systems. Sedimentology 60, 102–130. https://doi.org/10.1111/sed.12015.

Ashworth, P.J., Best, J.L., Jones, M.A., 2007. The relationship between channel avulsion, flow occupancy and aggradation in braided rivers: insights from an experimental model. Sedimentology 54, 497–513. https://doi.org/10.1111/j.1365-3091.2006.00845.x.

Aslan, A., Autin, W.J., Blum, M.D., 2005. Causes of river avulsion: insights from the Late Holocene avulsion history of the Mississippi River, U.S.A. Journal of Sedimentary Research 75, 650–664. https://doi.org/10.2110/jsr.2005.053.

Baker, P.A., Rigsby, C.A., Seltzer, G.O., Fritz, S.C., Lowenstein, T.K., Bacher, N.P., Veliz, C., 2001. Tropical climate changes at millennial and orbital timescales on the Bolivian Altiplano. Nature 409, 698–701. https://doi.org/10.1038/35055524.

Blard, P.H., Sylvestre, F., Tripati, A.K., Claud, C., Causse, C., Coudrain, A., Condom, T., Seidel, J.L., Vimeux, F., Moreau, C., Dumoulin, J.P., Lavé, J., 2011. Lake highstands on the Altiplano (Tropical Andes) contemporaneous with Heinrich 1 and the Younger Dryas: new insights from 14C, U-Th dating and δ18O of carbonates. Quaternary Science Reviews 30, 3973–3989. https://doi.org/10.1016/j.quascirev.2011.11.001.

Blum, M., Martin, J., Milliken, K., Garvin, M., 2013. Paleovalley systems: insights from Quaternary analogs and experiments. Earth Science Reviews 116, 128–169. https://doi.org/10.1016/j.earscirev.2012.09.003.

Brewer, C.J., Hampson, G.J., Whittaker, A.C., Roberts, G.G., Watkins, S.E., 2020. Comparison of methods to estimate sediment flux in ancient sediment routing systems. Earth Sci. Rev. 207, 103217. https://doi.org/10.1016/j.earscirev.2020.103217.

Bridge, J.S., Leeder, M.R., 1979. A simulation model of alluvial stratigraphy. Sedimentology 26, 617–644. https://doi.org/10.1111/j.1365-3091.1979.tb00935.x.

Bryant, M., Falk, P., Paola, C., 1995. Experimental study of avulsion frequency and rate of deposition. Geology 23, 365–368. https://doi.org/10.1130/0091-7613(1995)023<0365:ESOAFA>2.3.CO;2.

Cohen, S., Kettner, A.J., Syvitski, J.P.M., Fekete, B.M., 2013. WBMsed, a distributed global-scale riverine sediment flux model: model description and validation. Computational Geosciences 53, 80–93. https://doi.org/10.1016/j.cageo.2011.08.011.

Colombera, L., Mountney, N.P., Russell, C.E., Shiers, M.N., McCaffrey, W.D., 2017. Geometry and compartmentalization of fluvial meander-belt reservoirs at the bar-form scale: quantitative insight from outcrop, modern and subsurface analogues. Marine and Petroleum Geology 82, 35–55. https://doi.org/10.1016/j.marpetgeo.2017.01.024.

Costa, A.C., Bronstert, A., de Araújo, J.C., 2012. A channel transmission losses model for different dryland rivers. Hydrology and Earth System Sciences 16, 1111–1135. https://doi.org/10.5194/hess-16-1111-2012.

Costa, A.C., Foerster, S., de Araújo, J.C., Bronstert, A., 2013. Analysis of channel transmission losses in a dryland river reach in north-eastern Brazil using streamflow series, groundwater level series and multi-temporal satellite data. Hydrological Processes 27, 1046–1060. https://doi.org/10.1002/hyp.9243.

Dalman, R.A.F., Weltje, G.J., 2008. Subgrid parameterisation of fluvio–deltaic stratigraphy. Computational Geosciences 34, 1370–1380. https://doi.org/10.1016/j.cageo.2008.02.005.

Dalman, R.A.F., Weltje, G.J., 2012. SimClast: an aggregated forward stratigraphic model of continental shelves. Computational Geosciences 38, 115–126. https://doi.org/10.1016/j.cageo.2011.05.014.

Dalman, R.A.F., Weltje, G.J., Karamitopoulos, P., 2015. High-resolution sequence stratigraphy of fluvio–deltaic systems: prospects of system-wide chronostratigraphic correlation. Earth and Planetary Science Letters 412, 10–17. https://doi.org/10.1016/j.epsl.2014.12.030.

De Jong, M.G.G., Donselaar, M.E., Boerboom, H.T.W., Van Toorenenburg, K.A., Weltje, G.J., Van Borren, L., 2020. Long-range, high-resolution, stratigraphic correlation of Rotliegend fluvial-fan deposits in the central Dutch offshore. Marine and Petroleum Geology 119. https://doi.org/10.1016/j.marpetgeo.2020.104482.

de Lavenne, A., Skøien, J.O., Cudennec, C., Curie, F., Moatar, F., 2016. Transferring measured discharge time series: large-scale comparison of Top-kriging to geomorphology-based inverse modeling. Water Resources Research 52, 5555–5576. https://doi.org/10.1002/2016WR018716.

Donselaar, M.E., Cuevas Gozalo, M.C., Moyano, S., 2013. Avulsion processes at the terminus of semi-arid fluvial systems: lessons from the Río Colorado, Altiplano endorheic basin, Bolivia. Sedimentary Geology 283, 1–14. https://doi.org/10.1016/j.sedgeo.2012.10.007.

Donselaar, M.E., Cuevas Gozalo, M.C., Van Toorenenburg, K.A., Wallinga, J., 2022. Spatio-temporal reconstruction of avulsion history at the terminus of a modern dryland river system. Earth Surface Processes and Landforms 47, 1212–1228. https://doi.org/10.1002/esp.5311.

Edmonds, D.A., Hajek, E.A., Downton, N., Bryk, A.B., 2016. Avulsion flow-path selection on rivers in foreland basins. Geology 44, 695–698. https://doi.org/10.1130/G38082.1.

Fielding, C.R., Alexander, J., Allen, J.P., 2018. The role of discharge variability in the formation and preservation of alluvial sediment bodies. Sedimentary Geology 365, 1–20. https://doi.org/10.1016/j.sedgeo.2017.12.022.

Freeman, G.T., 1991. Calculating catchment area with divergent flow based on a regular grid. Computational Geosciences 17, 413–422. https://doi.org/10.1016/0098-3004(91)90048-I.

Friend, P.F., Slater, M.J., Williams, R.C., 1979. Vertical and lateral building of river sandstone bodies, Ebro Basin, Spain. Journal of the Geological Society 136, 39–46. https://doi.org/10.1144/gsjgs.136.1.0039.

Ganti, V., Chadwick, A.J., Hassenruck-Gudipati, H.J., Lamb, M.P., 2016. Avulsion cycles and their stratigraphic signature on an experimental backwater-controlled delta. Journal of Geophysical Research - Earth Surface 121, 1651–1675. https://doi.org/10.1002/2016JF003915.

Garreaud, R.D., Vuille, M., Clement, A.C., 2003. The climate of the Altiplano: observed current conditions and mechanisms of past changes. Palaeogeography,

Palaeoclimatology, Palaeoecology 194 (1–3), 5–22. https://doi.org/10.1016/S0031-0182(03)00269-4.
Gregory-Wodzicki, K.M., 2000. Uplift history of the Central and Northern Andes: a review. Geological Society of America Bulletin 112, 1091–1105. https://doi.org/10.1130/0016-7606(2000)112<1091:UHOTCA>2.0.CO;2.
Gouw, M., 2007. Alluvial architecture of fluvio-deltaic successions: a review with special reference to Holocene settings. Neth. J. Geosci. 86 (3), 211–227. https://doi.org/10.1017/S0016774600077817.
Hajek, E.A., Heller, P.L., Sheets, B.A., 2010. Significance of channel-belt clustering in alluvial basins. Geology 38 (6), 535–538. https://doi.org/10.1130/G30783.1.
Hajek, E.A., Edmonds, D.A., 2014. Is river avulsion style controlled by floodplain morphodynamics? Geology 42, 199–202. https://doi.org/10.1130/G35045.1.
Hajek, E.A., Wolinsky, M.A., 2012. Simplified process modeling of river avulsion and alluvial architecture: connecting models and field data. Sedimentary Geology 257-260, 1–30. https://doi.org/10.1016/j.sedgeo.2011.09.005.
He, Y., Bárdossy, A., Zehe, E., 2011. A review of regionalisation for continuous streamflow simulation. Hydrology and Earth System Sciences 15, 3539–3553. https://doi.org/10.5194/hess-15-3539-2011.
Heller, P.L., Paola, C., 1996. Downstream changes in alluvial architecture: an exploration of controls on channel stacking patterns. Journal of Sedimentary Research 66, 297–306. https://doi.org/10.1306/D4268333-2B26-11D7-8648000102C1865D.
Henares, S., Donselaar, M.E., Caracciolo, L., 2020. Depositional controls on sediment properties in dryland rivers: influence on near-surface diagenesis. Earth Science Reviews 208, 103297. https://doi.org/10.1016/j.earscirev.2020.103297.
Hoyal, D.C.J.D., Sheets, B.A., 2009. Morphodynamic evolution of experimental cohesive deltas. J. Geophys. Res. 114, F02009. https://doi.org/10.1029/2007JF000882.
Ielpi, A., Lapôtre, M.G.A., 2019. Barren meandering streams in the modern Toiyabe Basin of Nevada, U.S.A., and their relevance to the study of the pre-vegetation rock record. Journal of Sedimentary Research 89, 399–415. https://doi.org/10.2110/jsr.2019.25.
Ielpi, A., Lapôtre, M.G.A., Gibling, M.R., Boyce, C.K., 2022. The impact of vegetation on meandering rivers. Nature Reviews Earth Environment https://doi.org/10.1038/s43017-021-00249-6.
Jarihani, A.A., Larsen, J.R., Callow, J.N., McVicar, T.R., Johansen, K., 2015. Where does all the water go? Partitioning water transmission losses in a data-sparse, multi-channel and low-gradient dryland river system using modelling and remote sensing. Journal of Hydrology 529, 1511–1529. https://doi.org/10.1016/j.jhydrol.2015.08.030.
Jerolmack, D.J., Mohrig, D., 2007. Conditions for branching in depositional rivers. Geology 35, 463–466. https://doi.org/10.1130/G23308A.1.
Jones, H.L., Hajek, E.A., 2007. Characterizing avulsion stratigraphy in ancient alluvial deposits. Sedimentary Geology 202, 124–137. https://doi.org/10.1016/j.sedgeo.2007.02.003.
Jones, H.L., Schumm, S.A., 1999. Causes of avulsion: an overview. In: Smith, N.D., Rogers, J. (Eds.), Fluvial Sedimentology VI. Spec. Publ. Int. Assoc. Sedimentolvol. 28, pp. 171–178. https://doi.org/10.1002/9781444304213.ch13.
Karamitopoulos, P., Weltje, G.J., Dalman, R.A.F., 2014. Allogenic controls on autogenic variability in fluvio-deltaic systems: inferences from analysis of synthetic stratigraphy. Basin Research 26, 767–779. https://doi.org/10.1111/bre.12065.
Kelly, S.B., Olsen, H., 1993. Terminal fans-a review with reference to Devonian examples. Sedimentary Geology 85, 339–374. https://doi.org/10.1016/0037-0738(93)90092-J.
Kettner, A.J., Restrepo, J.D., Syvitski, J.P.M., 2010. A spatial simulation experiment to replicate fluvial sediment fluxes within the Magdalena River Basin, Columbia. Journal of Geology 118, 363–379. https://doi.org/10.1086/652659.
Kleinhans, M.G., Ferguson, R.I., Lane, S.N., Hardy, R.J., 2013. Splitting rivers at their seams: bifurcations and avulsion. Earth Surface Processes and Landforms 38, 47–61. https://doi.org/10.1002/esp.3268.
Knighton, A.D., Nanson, G.C., 1994. Flow transmission along an arid zone anastomosing river, Cooper Creek, Australia. Hydrological Processes 8, 137–154. https://doi.org/10.1002/hyp.3360080205.
Kraus, M.J., Aslan, A., 1999. Palaeosol sequences in floodplain environments: a hierarchical approach. In: Thiry, M., Simon-Coinçon, R. (Eds.), Palaeosol Sequences in Floodplain Environments: A Hierarchical Approach. Spec. Publ. Int. Assoc. Sedimentolvol. 27, pp. 303–321. https://doi.org/10.1002/9781444304190.ch12.
Lange, J., 2005. Dynamics of transmission losses in a large arid stream channel. Journal of Hydrology 306, 112–126. https://doi.org/10.1016/j.jhydrol.2004.09.016.
Leeder, M.R., 1978. A quantitative stratigraphic model for alluvium, with special reference to channel deposit density and interconnectedness. In: Miall, A.D. (Ed.), Fluvial Sedimentology. Can. Soc. Petrol. Geol. Mem.vol. 5, pp. 587–596.
Li, J., 2014. Terminal Fluvial Systems in a Semi-arid Endorheic Basin, Salar de Uyuni (Bolivia). Delft University of Technology, Delft, The Netherlands 978-90-8891-963-3 https://doi.org/10.4233/uuid:0dac02b5-7004-4aa4-99aa-237adadfab1f (Published Doctorate thesis, 164 pp.).
Li, J., Donselaar, M.E., Hosseini Aria, S.E., Koenders, R., Oyen, A.M., 2014. Landsat imagery-based visualization of the geomorphological development at the terminus of a dryland river system. Quaternary International 352, 100–110. https://doi.org/10.1016/j.quaint.2014.06.041.
Li, J., Luthi, M.E., Donselaar, M.E., Weltje, G.J., Prins, M.A., Bloemsma, M.R., 2015. An ephemeral meandering system river system: sediment dispersal processes in the Rio Colorado, Southern Altiplano Plateau, Bolivia. Zeitschrift für Geomorphologie 59, 301–317. https://doi.org/10.1127/zfg/2014/0155.
Li, J., Yang, X., Maffei, C., Tooth, S., Yao, G., 2018. Applying independent component analysis on Sentinel-2 imagery to characterize geomorphological responses to an extreme flood event near the non-vegetated Río Colorado terminus, Salar de Uyuni, Bolivia. Remote Sensing 10, 725. https://doi.org/10.3390/rs10050725.
Mackey, S.D., Bridge, J.S., 1995. Three-dimensional model of alluvial stratigraphy: theory and application. Journal of Sedimentary Research 65, 7–31. https://doi.org/10.1306/D42681D5-2B26-11D7-8648000102C1865D.
Makaske, B., Smith, D.G., Berendsen, H.J.A., 2002. Avulsions, channel evolution and floodplain sedimentation rates of the anastomosing upper Columbia River, British Columbia. Sedimentology 49, 1049–1071. https://doi.org/10.1046/j.1365-3091.2002.00489.x.
Meijer, X.D., 2002. Modelling the drainage evolution of a river–shelf system forced by Quaternary glacio-eustasy. Basin Research 14, 361–377. https://doi.org/10.1046/j.1365-2117.2002.00187.x.
Miall, A.D., 1996. The Geology of Fluvial Deposits. Springer, New York https://doi.org/10.1007/978-3-662-03237-4 (582 pp.).
Mohrig, D., Heller, P.L., Paola, C., Lyons, W.J., 2000. Interpreting avulsion process from ancient alluvial sequences; Guadalope–Matarranya system (northern Spain) and Wasatch Formation (western Colorado). Geological Society of America Bulletin 112, 1787–1803. https://doi.org/10.1130/0016-7606(2000)112<1787:IAPFAA>2.0.CO;2.
Morón, S., Amos, K.J., 2018. Downstream grain-size changes associated with a transition from single channel to anabranching. Sedimentology 65, 1590–1610. https://doi.org/10.1111/sed.12439.
Morón, S., Amos, K.J., Edmonds, D.A., Payenberg, T., Sun, X., Thyer, M., 2017. Avulsion triggering by El Niño–Southern Oscillation and tectonic forcing: the case of the tropical Magdalena River, Colombia. Geological Society of America Bulletin 129, 1300–1313. https://doi.org/10.1130/B31580.1.
Nicholas, A.P., Aalto, R.E., Sambrook Smith, G.H., Schwendel, A.C., 2018. Hydrodynamic controls on alluvial ridge construction and avulsion likelihood in meandering river floodplains. Geology 46, 639–642. https://doi.org/10.1130/G40104.1.
Nichols, G.J., Fisher, J.A., 2007. Processes, facies and architecture of fluvial distributary system deposits. Sedimentary Geology 195, 75–90. https://doi.org/10.1016/j.sedgeo.2006.07.004.
Nienhuis, J.H., Törnqvist, T.E., Esposito, C.R., 2018. Crevasse splays versus avulsions: a recipe for land building with levee breaches. Geophysical Research Letters 45, 4058–4067. https://doi.org/10.1029/2018GL077933.
North, C.P., Warwick, G.L., 2007. Fluvial fans: myths, misconceptions, and the end of the terminal-fan model. Journal of Sedimentary Research 77, 693–701. https://doi.org/10.2110/jsr.2007.072.
Phillips, J.D., 2011. Universal and local controls of avulsions in southeast Texas Rivers. Geomorphology 130, 17–28. https://doi.org/10.1016/j.geomorph.2010.10.001.
Powell, D.M., 2009. Dryland rivers: processes and forms. In: Parsons, A.J., Abrahams, A.D. (Eds.), Geomorphology of Desert Environments, 2nd ed. Springer Science+Business Media B.V., pp. 333–373 https://doi.org/10.1007/978-1-4020-5719-9 (12).
Reitz, M.D., Jerolmack, D.J., Swenson, J.B., 2010. Flooding and flow path selection on alluvial fans and deltas. Geophys. Res. Lett. 37, L06401. https://doi.org/10.1029/2009GL041985.
Romans, B.W., Castelltort, S., Covault, J.A., Fildani, A., Walsh, J.P., 2016. Environmental signal propagation in sedimentary systems across timescales. Earth-Science Reviews 153, 7–29. https://doi.org/10.1016/j.earscirev.2015.07.012.
Sheets, B.A., Hickson, T.A., Paola, C., 2002. Assembling the stratigraphic record: depositional patterns and time-scales in an experimental alluvial basin. Basin Research 14, 287–303. https://doi.org/10.1046/j.1365-2117.2002.00185.x.
Slingerland, R., Smith, N.D., 1998. Necessary conditions for a meandering-river avulsion. Geology 26, 435–438. https://doi.org/10.1130/0091-7613(1998)026<0435:NCFAMR>2.3.CO;2.
Slingerland, R., Smith, N., 2004. River avulsions and their deposits. Annual Review of Earth and Planetary Sciences 32, 257–285. https://doi.org/10.1146/annurev.earth.32.101802.120201.
Sømme, T.O., Martinsen, O.J., Lunt, I., 2013. Linking offshore stratigraphy to onshore paleotopography: the Late Jurassic–Paleocene evolution of the south Norwegian margin. Geological Society of America Bulletin 125, 1164–1186. https://doi.org/10.1130/B30747.1.
Stouthamer, E., Cohen, K.M., Gouw, M.J.P., 2011. Avulsion and its implications for fluvial–deltaic architecture: insights from the Holocene Rhine–Meuse delta. In: Davidson, S.K., Leleu, S., North, C.P. (Eds.), From River to Rock Record: The Preservation of Fluvial Sediments and Their Subsequent Interpretation. SEPM Spec. Publ.vol. 97, pp. 215–232. https://doi.org/10.2110/sepmsp.097.215.
Straub, K.M., Paola, C., Mohrig, D., Wolinsky, M.A., George, T., 2009. Compensational stacking of channelized sedimentary deposits. Journal of Sedimentary Research 79, 673–688. https://doi.org/10.2110/jsr.2009.070.
Syvitski, J.P.M., Milliman, J.D., 2007. Geology, geography and humans battle for dominance in the delivery of fluvial sediment to the coastal ocean. Journal of Geology 115, 1–19. https://doi.org/10.1086/509246.
Syvitski, J.P.M., Peckham, S.D., Hilberman, R.D., Mulder, T., 2003. Predicting the terrestrial flux of sediment to the global ocean: a planetary perspective. Sedimentary Geology 162, 5–24. https://doi.org/10.1016/S0037-0738(03)00232-X.
Thornes, J.B., 2009. Catchment and channel hydrology. In: Parsons, A.J., Abrahams, A.D. (Eds.), Geomorphology of Desert Environments, 2nd ed. https://doi.org/10.1007/978-1-4020-5719-9_11 (831 pp.).
Van Dijk, M., Postma, G., Kleinhans, M.G., 2009. Autocyclic behaviour of fan deltas: an analogue experimental study. Sedimentology 56, 1569–1589. https://doi.org/10.1111/j.1365-3091.2008.01047.x.
Van Toorenenburg, K.A., 2018. The Key Role of Crevasse Splays in Prograding River Systems - Analysis of Evolving Floodplain Accommodation and Its Implications for Architecture and Reservoir Potential. Delft University of Technology, Delft, The Netherlands 978-94-6366-084-6 (Published Doctorate thesis, 122 pp.).
Van Toorenenburg, K.A., Donselaar, M.E., Noordijk, N.A., Weltje, G.J., 2016. On the origin of crevasse-splay amalgamation in the Huesca fluvial fan (Ebro Basin, Spain): implications for connectivity in low-net-to-gross fluvial deposits. Sedimentary Geology 343, 156–164. https://doi.org/10.1016/j.sedgeo.2016.08.008.
Van Toorenenburg, K.A., Donselaar, M.E., Weltje, G.J., 2018. The life cycle of crevasse splays as a key mechanism in the aggradation of alluvial ridges and river avulsion.

Earth Surface Processes and Landforms 43, 2409–2420. https://doi.org/10.1002/esp.4404.

Wang, J., Plink-Björklund, P., 2019. Stratigraphic complexity in fluvial fans: Lower Eocene Green River Formation, Uinta Basin, USA. Basin Research 31, 892–919. https://doi.org/10.1111/bre.12350.

Wang, Y., Straub, K.M., Hajek, E.A., 2011. Scale-dependent compensational stacking: an estimate of autogenic time scales in channelized sedimentary deposits. Geology 39, 811–814. https://doi.org/10.1130/G32068.1.

Weight, R.W., Anderson, J.B., Fernandez, R., 2011. Rapid mud accumulation on the Central Texas shelf linked to climate change and sea-level rise. Journal of Sedimentary Research 81, 743–764. https://doi.org/10.2110/jsr.2011.57.

Zhang, J., Covault, J., Pyrcz, M., Sharman, G., Carvajal, C., Milliken, K., 2018. Quantifying sediment supply to continental margins: application to the Paleogene Wilcox Group, Gulf of Mexico. AAPG Bulletin 102, 1685–1702. https://doi.org/10.1306/01081817308.